Catal Lett (2008) 121:121–130
DOI 10.1007/s10562-007-9308-1

Sinusoidal Perturbation of the Oscillatory Kinetics of the $N_2O + H_2$ Reaction on Ir(110)

Mari Carmen Lemos · Antonio Córdoba

Received: 5 September 2007 / Accepted: 9 October 2007 / Published online: 4 December 2007

Abstract The model, proposed by Peskov et al. (Catal Today 105:223, 2005) to describe kinetic oscillations observed in the $N_2O + H_2$ reaction on Ir(110), is used to illustrate the effect of periodic perturbation of the reactant pressures on oscillations. The attention is focused on the conversion of natural period-1 oscillations to period-1 oscillations with the imposed frequency. For this conversion, simultaneous perturbation of both reactant pressures is found to be much more efficient compared to perturbation of one of the pressures.

Keywords Heterogeneous catalysis · Oscillatory reaction · Periodic forcing · Model of surface chemical reaction · Reduction of N_2O by H_2

1 Introduction

The periodical perturbation of the kinetics of a reaction by the variation of some external control parameter such as, for example, the pressure of one of the reactants or the temperature of the gas, is one of the frequently used tools in the study of heterogeneous catalytic processes [1]. Results obtained in this field generally refer to perturbation of oscillations of period-1 (P1) by means of periodical modulation of one of the control parameters. In experiments focused on the study of the complex behavior of oscillatory catalytic reactions, the technique of periodical forcing is used as well in order to stabilize oscillations P1 (we obtain this if external and internal frequencies coincide) or to generate quasi-periodical oscillations or to control chaos.

Autonomous isothermal oscillations in the reaction rates of the reaction $N_2O + H_2$ on the surface of Ir(110) [2] have been reported recently. The products of the reaction are N_2 and H_2O. The rate oscillations are found in a narrow range of temperature between 460 and 464 K, for ratios between partial pressures p_{H_2}/p_{N_2O} close to 1. The period of the oscillations is nearly 60 s. The oscillatory behavior in this system is special due to the unusual phase difference in the kinetic oscillations of the reaction products. Thus, N_2 oscillates in counter-phase with the reactant N_2O, and the maxima of the oscillations of H_2O are "delayed" compared with the maxima of the oscillations of N_2. Later, Peskov et al. [3, 4] developed, successfully enough, a mean field (MF) mathematical model that describes the oscillatory behavior experimentally observed and that explains the origin of the phase difference between both the kinetic oscillations of N_2 and H_2O. They demonstrated that the unusual phase difference between the oscillations of the two reaction products can be explained on the basis of the character of the lateral interactions between the adsorbed species.

The purpose of this study is to analyse the influence that the technique of periodical forcing, which we have previously applied to the reaction of the catalytic oxidation of CO [5, 6], has on the oscillatory behavior found in the reaction $N_2O + H_2$, starting from the MF model proposed by Peskov et al. In this case, due to the presence of two reactants, partial pressures in each of them can be perturbed simultaneously, following the guidelines of Zhdanov and Kasemo [7], which perturbed the kinetic oscillations generated from a generic model proposed by Sales et al. [8] for the oxidation of CO on Pt with formation of surface oxide.

M. C. Lemos (✉) · A. Córdoba
Departamento de Física de la Materia Condensada,
Universidad de Sevilla, P. O. Box 1065, Sevilla 41080, Spain
e-mail: lemos@us.es

This paper is divided as follows. The characteristics and the results of the non-perturbed model are explained in Sect. 2. In Sect. 3 we show the results of this study of the periodical forcing applied to the periodical oscillations generated in the model proposed by Peskov et al. and we show how efficient periodical forcing can be when we want to convert autonomous oscillations P1 exhibited experimentally to oscillations P1 with the external frequency. Finally, in Sect. 4 we summarize the conclusions and highlight the most relevant points of this paper.

2 The Model

The mechanism of the reaction includes the following steps: adsorption/desorption of N_2O and H_2, dissociation of N_2O, and formation of H_2O. We assume that the reaction products N_2 and H_2O are immediately desorbed after their formation on the catalytic surface.

$$N_2O\,(g) + V \xrightarrow{k_1} N_2O\,(ads) \tag{1}$$

$$N_2O\,(ads) \xrightarrow{k_{-1}} N_2O\,(g) + V \tag{2}$$

$$H_2\,(g) + 2\,V \xrightarrow{k_2} 2\,H\,(ads) \tag{3}$$

$$2\,H\,(ads) \xrightarrow{k_{-2}} H_2\,(g) + 2\,V \tag{4}$$

$$N_2O\,(ads) \xrightarrow{k_3} N_2\,(g) + O\,(ads) \tag{5}$$

$$O\,(ads) + 2\,H\,(ads) \xrightarrow{k_4} H_2O\,(g) + 3\,V \tag{6}$$

where (g) indicates the gaseous phase, (ads) denotes an adsorbed particle on the surface, and V is a vacant site in the lattice. The mathematical modelization is done at a macroscopic level and is based on the standard MF approximation. So, the set of coupled non-linear equations describing the time change of the densities of the adsorbed particles is:

$$\frac{dn_{N_2O}}{dt} = k_1\,p_{N_2O}\,(1 - n_{N_2O} - n_O) - k_{-1}\,n_{N_2O} - k_3\,n_{N_2O} \tag{7}$$

$$\frac{dn_O}{dt} = k_3\,n_{N_2O} - k_4\,n_O\,n_H^2 \tag{8}$$

$$\frac{dn_H}{dt} = k_2\,p_{H_2}\,(1 - n_H)^2 - k_{-2}\,n_H^2 - k_4\,n_O\,n_H^2 \tag{9}$$

where n_{N_2O}, n_O and n_H are the densities of adsorbed particles N_2O, O and H, respectively. The model assumes as well that N_2O and H_2 are adsorbed on separate sublattices and that, therefore, $n_V + n_{N_2O} + n_O = 1$ and $n_V + n_H = 1$ for each sublattice. Moreover, variations of the partial pressures p_{N_2O} and p_{N_2} are very small during the reaction. The rate constants k_i ($i = \pm1, \pm2, 3, 4$) are assumed in the Arrhenius form.

The numerical analysis of the set of Eqs. 7–9 does not reveal solutions of the kind of limit cycle for a wide range of k_i. To obtain oscillations we need to introduce in the model lateral interaction between adatoms. It follows from the analysis of thermal desorption spectra that oxygen greatly modifies the desorption and dissociation rates of N_2O, and then we assume that, due to lateral interaction, the adsorbed oxygen increases the desorption and dissociation rates of N_2O.

Thus, on the basis of the available experimental data, it is assumed that the rate constants k_{-1} and k_3 depend on the surface coverage of oxygen: $k_{-1} = k_{-1}^*\,\exp(e_{-1}n_O)$ and $k_3 = k_3^*\,\exp(e_3 n_O)$. So, the values of the parameter of the model were selected so that they produce the most similarity between the solutions of the model and the experimental data: $k_1 = 6.2 \times 10^4\ s^{-1}\ mbar^{-1}$, $k_{-1}^* = 0.001\ s^{-1}$, $k_2 = 8.3 \times 10^5\ s^{-1}\ mbar^{-1}$, $k_{-2} = 0.003\ s^{-1}$, $k_3^* = 0.014\ s^{-1}$, $k_4 = 0.225\ s^{-1}$, $p_{N_2O} = 10^{-6}$ mbar, $p_{H_2} = 1.2 \times 10^{-6}$ mbar, $e_{-1} = 4$, and $e_3 = 10$, data obtained at temperature 460 K.

Figure 1 top shows the oscillations P1 of the coverages of the species adsorbed, and Fig. 1 bottom shows the oscillations in the rates of the processes of adsorption-desorption of N_2O, formation of H_2O, and dissociation of N_2O. This last value coincides with the rate of formation of N_2, because according to the experimental data the molecules N_2 desorb immediately after their formation on the catalytic surface. These oscillations are obtained from the time series resulting from the solution of the kinetic Eqs. 7–9 by the method of Runge–Kutta. It can be observed that N_2 oscillates with some phase difference with regard to N_2O and the maxima of the formation of H_2O are slightly delayed compared to the maxima of the formation N_2. We must indicate here that, during the first stage of the time evolution, oscillations of N_2(g) are in counter-phase with those of N_2O (ads) and the maxima of H_2O(g) are delayed in relation to the maxima of N_2(g). These facts are reported in Refs. [3] and [4]. However, as time increases, the phase difference between both oscillations gets smaller, as Fig. 1 shows. The origin of this time delay is related to the counter-phase that is observed in the concentration of O with regard to that of N_2O. The mechanism of the oscillations can be explained as follows: starting from a clean surface, hydrogen immediately occupies all the sites in the sublattice and, therefore, it plays a minor role in the appearance of oscillations. Concentration of N_2O on the surface keeps growing. Due to the dissociation of N_2O, the concentration of adsorbed oxygen increases as well. Oxygen accelerates dissociation of N_2O and surface concentration decreases drastically, while the oxygen coverage increases in an autocatalytic way. However,

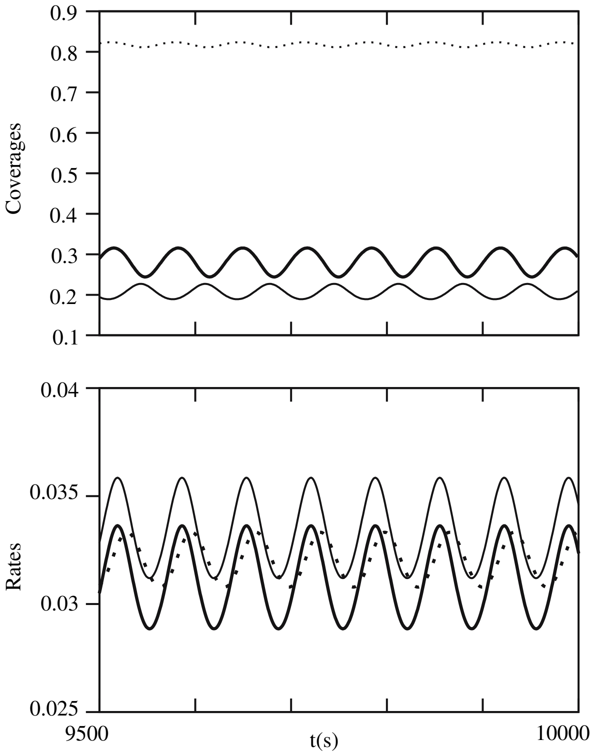

Fig. 1 Autonomous oscillations P1 of the coverages n_H (dashed line), n_{N_2O} (thick line) and n_O (thin line) (top of figure), and of rates of dissociation of n_{N_2O} (thin line), of the adsorption-desorption of n_{N_2O} (dashed line) and of the formation of H_2O (thick line) (bottom of figure)

concentration of surface oxygen begins to diminish because of its reaction with hydrogen. The decrease of the concentration of oxygen leads to an increase of the surface concentration of N_2O. As a result of this process the dissociation rate of N_2O increases again, leading to an increase of the surface concentration of oxygen. Oxygen accelerates the dissociation rate of N_2O again and the cycle of oscillations begins anew.

Figure 2 shows in more detail the natural oscillations P1 of the densities of adatoms (Fig. 1 top) obtained from the model. The periodical regime is represented qualitatively by the Poincaré map enclosed: the points are located on the same perfectly defined closed curve. The Fourier spectrum is discrete and shows a fundamental frequency: $f_0 = 0.01489$ Hz, since the second peak corresponds to its harmonic $2f_0 = 0.02978$ Hz. The period of the autonomous oscillation, 67 s, is very close to that obtained from experiments (60 s).

3 Results of the Perturbed Model

To test the stability of the oscillatory behavior found in the model, a perturbation in the partial pressure of the gases N_2O and H_2 is applied, using a sinusoidal function with only one frequency:

$$p^*_{N_2O} = p_{N_2O}[1 + A\sin(2\pi f t)] \; ; \qquad p^*_{H_2} = p_{H_2}[1 + B\sin(2\pi f t + \varphi)]$$

where A (or B) is the normalized amplitude, f is the frequency and φ is the initial phase difference between both perturbations. A systematic variation of A and/or B allows us to draw the kinetic phase diagram of the perturbed model that shows the dynamics states of the system and its possible bifurcation points. The values of the other parameters of the perturbed model are the same that those of the previous section. Most periodical modulations are performed changing only one control parameter and, nevertheless, in most realistic reactions two or more reactants participate; hence it is neccesary to control simultaneously two or more parameters; in this paper two external

Fig. 2 Time series of natural oscillations of coverages of H, N_2O, and O, obtained from mean field equations of the kinetic model. Both the time series and the Poincaré maps, along with the Fourier spectra attached, show behavior P1. The fundamental frequency corresponds to the peak $f_0 = 0.01489$ Hz, the value 0.02978 being its harmonic

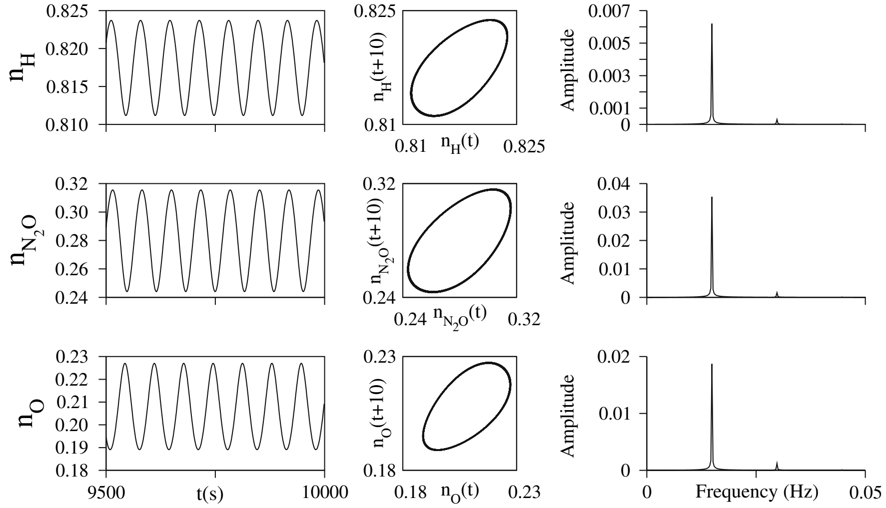

parameters—partial pressure of N_2O and H_2- are perturbed simultaneously.

To simplify the presentation of results, n_{N_2O} is chosen as the only output variable. In general, the time series obtained have 40,000 time steps (100,000 when the system is close to critical lines) and it is observed that, at the begining, during a transitory stage, all the perturbed oscillations have an irregular form. During this stage, the internal dynamics and the external perturbation adjust to each other until, as time increases, the system relaxes and exhibits well defined oscillations. The duration of the transitory stage becomes shorter as the amplitude of the modulation increases, whenever the system is far from the critical lines. When the system reaches the region of oscillations P1 at the external frequency, the transitory stage diminishes considerably. Therefore, the 30,000 first points are neglected in order to fully remove the transitory regime in all the cases and with the remaining 10,000 points we calculate the time average of n_{N_2O} and its fluctuation, so that $n_{N_2O} = \langle n_{N_2O} \rangle + \theta$. Results are analysed using the fluctuation of the surface density of N_2O. Afterwards, a thorough study of the time series obtained is performed using typical tools of non-linear dynamics and calculating, among other quatities, the Fourier transform.

Six kinds of perturbations have been analyzed, depending on whether only one or both partial pressures of the reactants are perturbed: (i) Perturbation of pressure p_{N_2O} ($A \neq 0$ and $B = 0$); (ii) perturbation of pressure p_{H_2} ($A = 0$ and $B \neq 0$, with $\varphi = 0$); perturbation of both pressures for values (iii) $A = B$ and $\varphi = 0$; (iv) $A = B$ and $\varphi = \pi/2$; (v) $A = B$ and $\varphi = \pi$; and (vi) $A = B$ and $\varphi = 3\pi/2$.

It is convenient to remember that, up to a certain point, the behavior of the periodically perturbed oscillatory system is general [9]. When forcing happens at a low amplitude, these systems usually exhibit a region of quasi-periodical oscillations. Inside this region are incrusted a number of island (the so-called *Arnold tongues*) of periodical evolution that correspond to the cases in which the ratio between the forced and natural frequencies, f/f_0, is close to an integer or to one simple fraction (in the practice, only the major tongues can be located). As the amplitude of the perturbations increases, it is possible sometimes to observe regular oscillations, which are oscillations modulated with a period significantly bigger than both natural and imposed periods. The regions where these periodical oscillations are observed are called synchronization bands between the system and the perturbation. The wideness of a synchronization band, that is, the range of frequency where the response of the perturbed system is periodical for a fixed value of the normalized amplitude, increases as the amplitude of the modulation increases. Chaotic oscillations can be observed as well when the amplitude of the perturbations increases; in this case the transition to chaos takes place by means of the duplication of period. Finally, if the amplitude of the sinusoidal forcing increases, a train of waves harmonic is obtained, that is to say, stable limit cycles which represent oscillations P1 with the frequency imposed.

To characterize the effect of different perturbations on the natural oscillations found in the model and to show the efficiency of the perturbations with regard to the conversion of natural oscillations to oscillations P1 with the frequency imposed, we have drawn six kinetic phase diagrams (Fig. 3), corresponding to the perturbations mentioned above. The internal areas drawn in terms of the normalized amplitude and the frequency of forcing represent, for each diagram, the regions of forced oscillations P1 with the imposed frequency. These results are qualitative: a complete classification including the *Arnold tongues* or other kind of regime different of that shown here is outside of the aim of this paper. The results obtained indicate that, in general, the simultaneous perturbation of the pressures p_{N_2O} and p_{H_2} (Fig. 3b) are more efficient than those in which only one partial pressure is perturbed (Fig. 3a). In this case, perturbations of kind (ii) are sligthly more efficient than those of kind (i), because the range of external frequencies that are resonant with the perturbed dynamical system is wider. For perturbations in which the normalized amplitudes of the partial pressures of N_2O and H_2 are equal ($A = B$, Fig. 3b), the phase diagrams are similar. This feature can be observed in more detail in Fig. 4, which collects the cases (iii), (iv), (v) and (vi) included in Fig. 3b. The greatest efficiency is found for perturbations of the kind (iv) ($A = B$, $\varphi = \pi/2$). In this case,

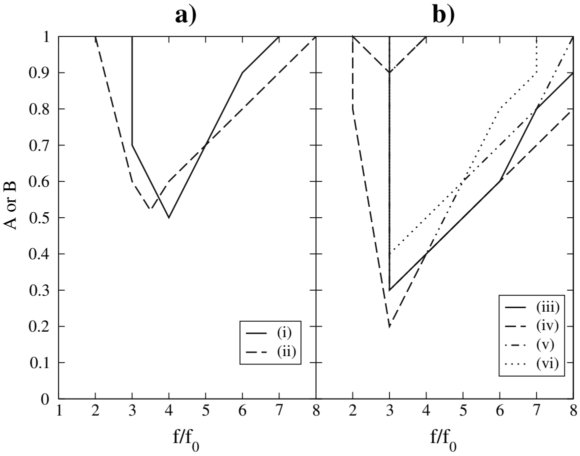

Fig. 3 Kinetic phase diagram obtained by periodical perturbations of the model in function of the normalized amplitude (*A* or *B*) and the frequency *f* of the perturbation, $f_0 = 0.01489$ Hz being the autonomous frequency. (**a**) (i) Perturbation of p_{N_2O}, with $A \neq 0$, $B = 0$); (ii) perturbation of p_H, with $A = 0$, $B \neq 0$ and $\varphi = 0$, (**b**) Simultaneous perturbation of p_{N_2O} and p_{H_2}, with $A = B$: (iii) $\varphi = 0$; (iv) $\varphi = \pi/2$; (v)($\varphi = \pi$ (vi) $\varphi = 3\pi/2$. The areas inside the curves correspond to regions of oscillations P1 at the perturbation frequency and they are peninsulas in the sea of other periodical regimes

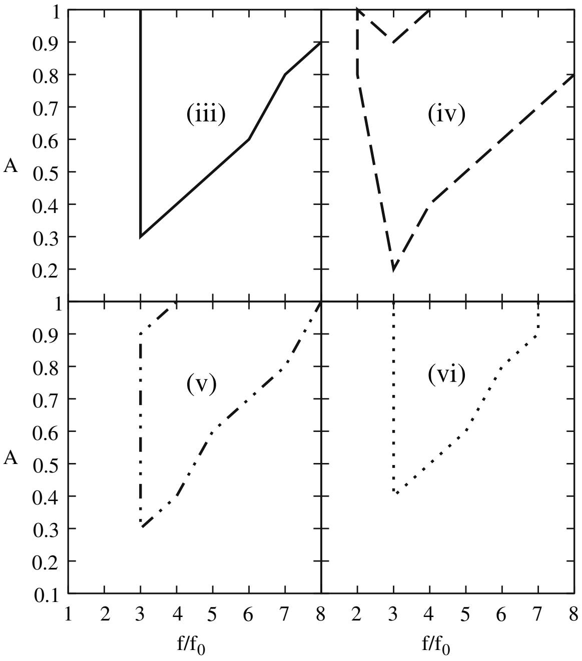

Fig. 4 Details of the kinetic phase diagram of the perturbed model corresponding to Fig. 3b. It can be seen here that the extension of the region of oscillations P1 with the external frequency *f* disminishes in the order (iv), (iii), (v) and (vi). The top zone in the diagram (iv), corresponding to high values of the normalized amplitude, is a region of oscillations P2 at the external frequency *f*

the beginning of the region corresponding to forced oscillations P1 with external frequency *f* is located at an amplitude of modulation smaller than the remaining cases shown in Fig. 4. Besides, the area of the harmonic waves oscillating at the imposed frequency is the biggest one of all the cases presented. We think that this fact is due to perturbations of the partial pressures $p^*_{N_2O} = p_{N_2O}[1 + A\sin(2\pi ft)]$ and $p^*_{H_2} = p_{H_2}[1 + A\cos(2\pi ft + \varphi)]$ are in counter-phase, favoring the characteristics of the non-perturbed model, and oscillations P1 with the natural frequency convert easily to oscillations P1 with the imposed frequency.

Some general issues can be extracted from the diagrams shown in Figs. 3 and 4:

1) At a frequency smaller than $f_0, f < f_0$, the technique of periodical forcing cannot convert the natural oscillations P1 to oscillations P1 with the external frequency *f*. For perturbations $f < f_0$, natural oscillations become oscillations with period-2 (P2), first at a frequency f_0 and next, as *A* increases, at frequency *f*. The kind of periodicity P1, P2, ... P*n* is established taking into account the number of maxima n by period of n_{N_2O}.
2) Natural oscillations are stable if external frequency equalizes the internal one, $f = f_0$. The shape of oscillations P1 at f_0 depends on the amplitude of the modulation. It should be pointed out that they are observed even with the maximum value of the normalized amplitude ($A = 1$), taking into account that the amplitude of the oscillation increases as *A* increases.
3) For perturbations with $f = 2f_0$, natural oscillations change to oscillations with different periodicity (P1, P2, and even period-3 (P3)) at frequency f_0. The range from P1 to P3 is obtained increasing the normalized amplitude. There are two exceptions to this rule: these oscillations with different periodicity at frecuency f_0 become oscillations P1 at the imposed frequency ($2f_0$) for the case (ii) (for $A = 1$) and for the case (iv) (for $A \geq 0.8$).
4) For perturbations with $f \geq 3f_0$, natural oscillations can become easily oscillations P1 with the imposed frequency *f*. It can be seen in each diagram that the width of band of the harmonic wave train increases as the amplitude of the modulation increases. Outside the region of oscillations P1 at external frequency *f*, oscillations P1 at natural frequency are found, increasing their periodicity as the perturbing amplitude increases. If A goes on increasing, oscillations with a periodicity greater than 1 and with the external frequency *f* are obtained. And if A continues increasing, the periodicity of the oscillations keeps diminishing until it reaches the region of oscillations P1 at frequency *f*. This behavior is observed for each fixed value of *f*.

With regard to the time average of n_{N_2O}, $\langle n_{N_2O} \rangle$, one can observe, for a fixed value of f, the following behavior:

5) When only p_{N_2O} is perturbed (case (i)), although the average $\langle n_{N_2O} \rangle$ increases slightly as *A* increases, it remains practically constant for all the frequencies tested.
6) The results of the perturbations of p_{H_2} (case (ii)) contrast with the preceding case and are similar to those shown in Fig. 4. For $f < f_0$ and $f = 2f_0$, $\langle n_{N_2O} \rangle$ increases at first and later on diminishes as *A* increases. For $f = 3f_0$, $\langle n_{N_2O} \rangle$ diminishes as *A* increases, for the cases (ii), (iii) and (iv); however, for the cases (v) and (vi), $\langle n_{N_2O} \rangle$ increases at first and later on it decreases. Finally, for all the cases in which $B \neq 0$ for $f \geq 4f_0$, $\langle n_{N_2O} \rangle$ decreases as *A* increases.

Next, Figs. 5 and 6 show some time series of the forced oscillations of n_{N_2O} for the cases (i) ($A \neq 0$, $B = 0$) and (iv) ($A = B$, $\varphi = \pi/2$), respectively, which manifest some ideas previously stated. In these figures we show the behavior of the model when it is perturbed for the four external frequencies: (a) $f_1 = 0.5f_0$, (b) $f_2 = 2f_0$, (c) $f_3 = 4f_0$, and (d) $f_4 = 6f_0$, $f_0 = 0.01489$ Hz being the natural

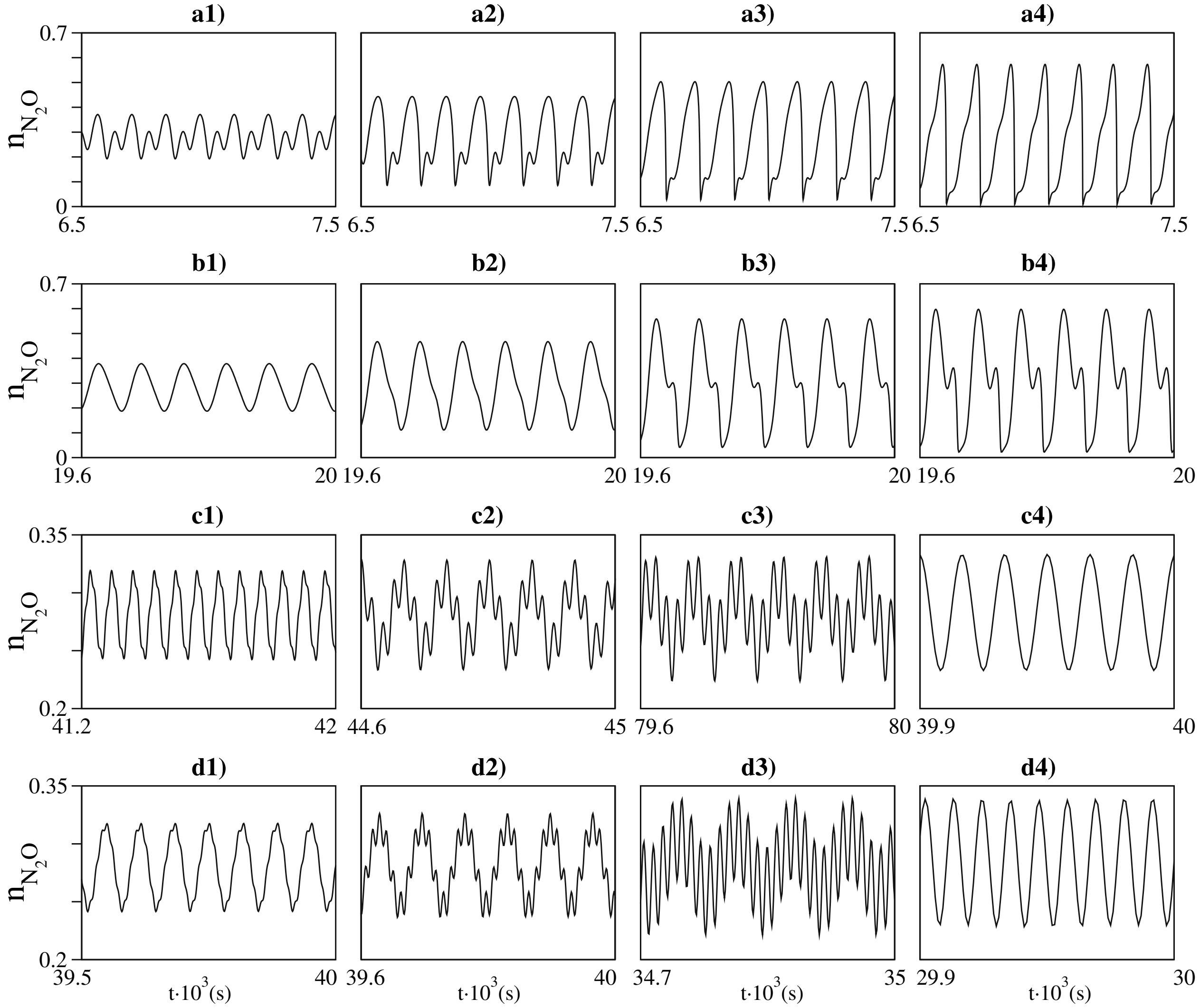

Fig. 5 Time series of the forced oscillations of the coverage of N_2O for $A \neq 0$ and $B = 0$ (case (i). For $f_1 = 0.5f_0$: (**a1**) $A = 0.05$, oscillations P2 at frecuency f_0; (**a2**) $A = 0.2$, oscillations P2 at the imposed frecuency f_1; (**a3**) $A = 0.4$, P2 at f_1; (**a4**) $A = 0.7$, P2 at f_1. For $f_2 = 2f_0$: (**b1**) $A = 0.05$, P1 at f_0; (**b2**) $A = 0.2$, P1 at f_0; (**b3**) $A = 0.5$, P2 at f_0; (**b4**) $A = 0.7$, P2 at f_0. For $f_3 = 4f_0$: (**c1**) $A = 0.05$, P1 at f_0; (**c2**) $A = 0.2$, P4 at f_0; (**c3**) $A = 0.3$, P4 at f_3; (**c4**) $A = 0.5$, P1 at f_3. For $f_4 = 6f_0$: (**d1**) $A = 0.05$, P1 at f_0; (**d2**) $A = 0.2$, P6 at f_0; (**d3**) $A = 0.6$, P7 at f_4; (**d4**) $A = 0.9$, P1 at f_4. The kind of periodicity P1, P2, ... P*n* is established taking into account the number of maxima n by period of n_{N_2O}

frequency. Although both figures are similar, there are some differences. So, Fig. 5 shows the increase—although sometimes it is a slight one of the amplitude of the oscillations as the amplitude of the modulation A increases (from left to right), although the time average $\langle n_{N_2O} \rangle$ remains practically constant. This fact appears for all the frequencies tested. However, Fig. 6 shows that for the cases (c) $f_3 = 4f_0$, and d) $f_4 = 6f_0$, the amplitude diminishes from A certain value of A. One can point out as well that for (b) $f_2 = 2f_0$ in the case (i) (Fig. 5) perturbed oscillations P1 and P2 at frequency f_0 are observed as A increases. However, for the case (iv) (Fig. 6) oscillations P1 at the imposed frequency appear, as it can be observed for the case b4, in which $A = 0.8$. This is the amplitude of perturbation necessary for the beginning of perturbed oscillations P1 at the forcing frequency. The other cases shown in Fig. 6 indicate this beginning for $A = 0.4$ (c4) and $A = 0.6$ (d4), while in Fig. 5 this fact happens for $A = 0.5$ (c4) and $A = 0.9$ (d4). The remaining cases shown in Figs. 5 and 6 are similar. So, for $f_1 = 0.007445$ Hz, the perturbation converts the natural oscillation P1 to oscillations P2, with the natural frequency (case a1) or with the imposed frequency (cases a2, a3 and a4). When the external frequency duplicates the natural one, $f_2 = 0.02978$ Hz, natural oscillations are stable enough for low amplitude, and oscillations P1 with the natural frequency result (cases b1 and b2). However, they become oscillations P2 with frequency f_0 when amplitude increases

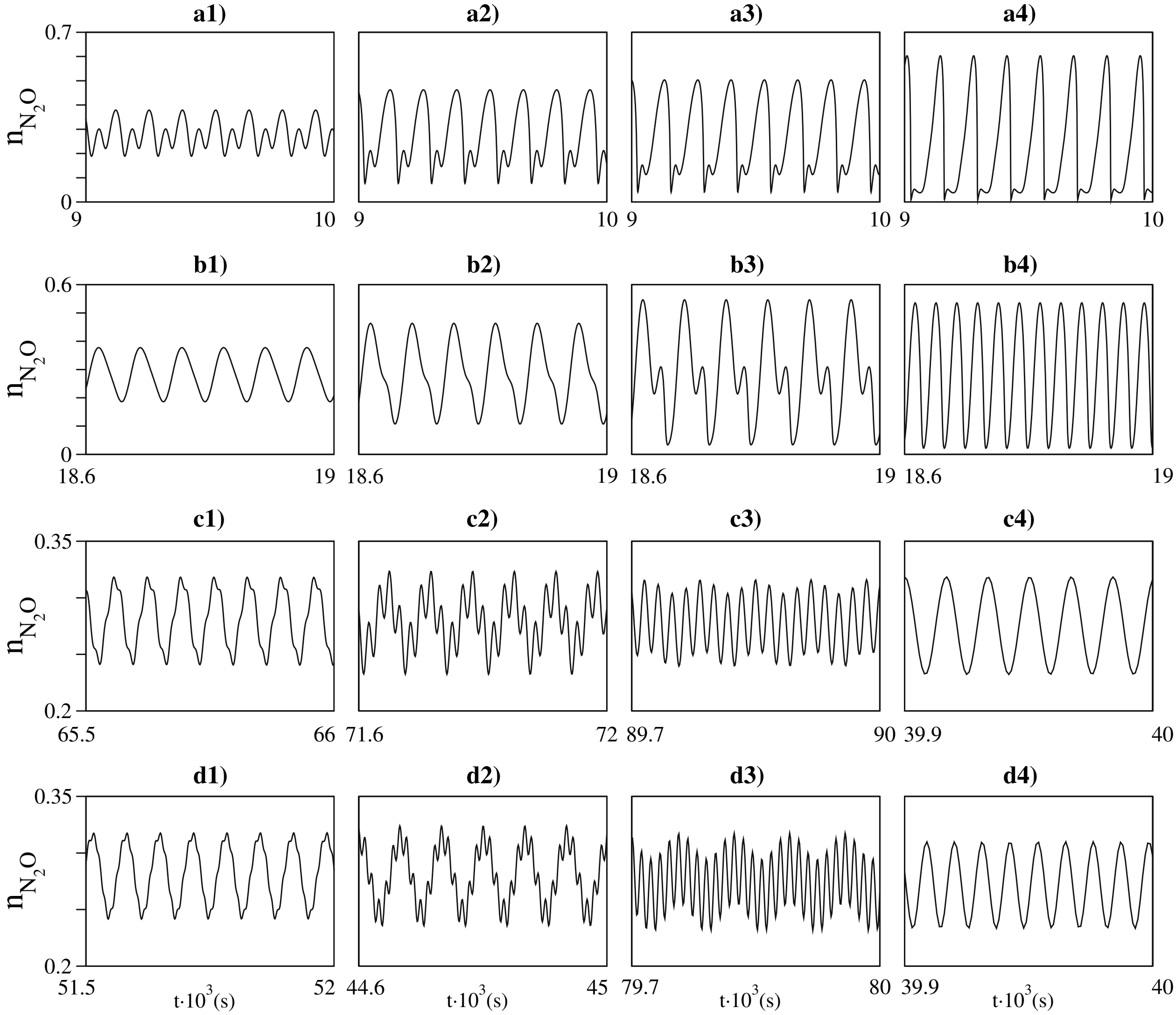

Fig. 6 Time series of the forced oscillations of the coverage of N_2O for $A = B$ and $\varphi = \pi/2$ (case (iv)). For $f_1 = 0.5 f_0$: (**a1**) A = 0.05, oscillations P2 at frecuency f_0; (**a2**) $A = 0.2$, oscillations P2 at the imposed frecuency f_1; (**a3**) A = 0.3, P2 at f_1; (**a4**) $A = 0.7$, P2 at f_1. For $f_2 = 2 f_0$: (**b1**) $A = 0.05$, P1 at f_0; (**b2**) $A = 0.2$, P1 at f_0; (**b3**) $A = 0.5$, P2 at f_0; (**b4**) $A = 0.8$, P1 at f_2. For $f_3 = 4 f_0$: (**c1**) $A = 0.05$, P1 at f_0, (**c2**) $A = 0.2$, P4 at f_0; (**c3**) $A = 0.3$, P5 at f_3; (**c4**) $A = 0.4$, P1 at f_3. For $f_4 = 6 f_0$: (**d1**) $A = 0.05$, P1 at f_0; (**d2**) $A = 0.2$, P5 at f_0; (**d3**) $A = 0.5$, P7 at f_4; (**d4**) $A = 0.6$, P1 at f_4

(case b3). If the normalized amplitude keeps increasing, oscillations P2 with f_0 sustain in the case b4 of Fig. 5 or they become oscillations P1 at an external frequency $f_2 = 0.02978$ Hz, like the case b4 in Fig. 6. In the third case, for $f_3 = 0.05956$ Hz and $A = 0.05$ (case c1), the perturbed system exhibits oscillations P1 with the natural frequency. However, when the perturbing amplitude increases, it displays oscillations period-4 (P4) (case c2), and, if A goes on increasing, the system ends up oscillating with P1 at the imposed frequency ($f_3 = 0.05956$ Hz). The fourth case, for $f_4 = 0.08934$ Hz, is similar to the third one. For the case d4 the regime of periodical oscillations that oscillate with the perturbing frequency is reached. We want to highlight that the passage from natural oscillations P1 at natural frequency f_0 to forced oscillations P1 at the external frequency f takes place through the appearance of oscillations with multiple periodicity, oscillating at frequency f_0 or at frequency f, depending, for a fixed value of the perturbing frequency, on the increase of the amplitude of the modulation A.

The following four figures summarize the most representative perturbed oscillatory states obtained: (1) Figure 7, for $A = B$, $\varphi = \pi$, with $f = 2 f_0 = 0.02978$ Hz, and $A = 0.8$, oscillations P2 at the internal frequency f_0 result, (2) Figure 8, for $A = B$, $\varphi = 0$, with $f = 4 f_0 = 0.05956$ Hz, and $A = 0.2$, oscillations P4 at the internal frequency f_0 are obtained, (3) Figure 9, for $A = B$, $\varphi = \pi/2$, with $f = 0.5 f_0 = 0.007445$ Hz, and $A = 0.3$, oscillations P2 at

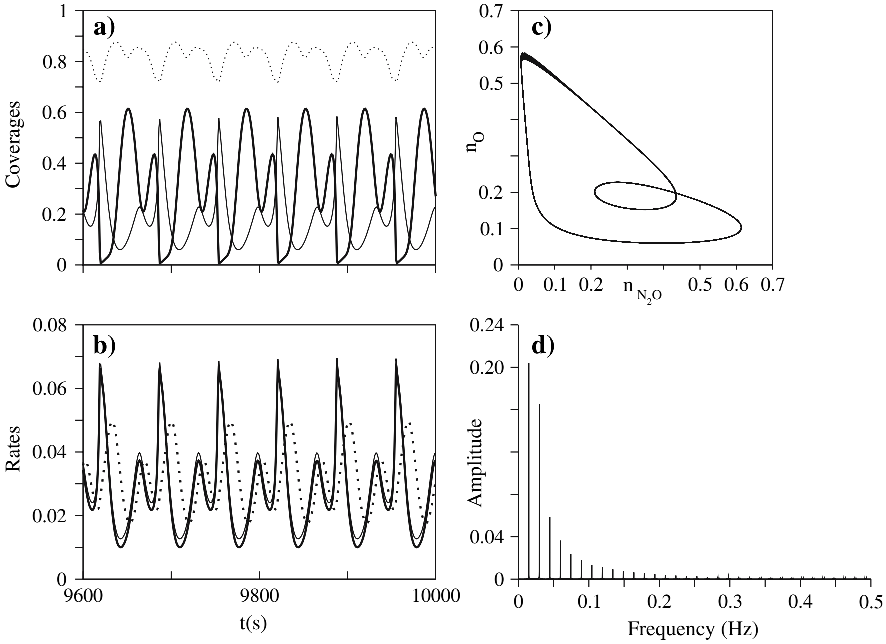

Fig. 7 Forced oscillations P2 at the natural frequency f_0 obtained for the case (v), $A = B$ and $\varphi = \pi$, with $A = 0.8$ and the imposed frequency $f = 2f_0$. (**a**) Time series of the coverages n_H (dashed line), n_{N_2O} (thick line) and n_O (thin line), (**b**) Time series of the rates of dissociation of N_2O (thin line), of adsorption-desorption of N_2O (dashed line) and of formation of H_2O (thick line), (**c**) Stable limit cycle, (**d**) Discrete Fourier spectrum. The system exhibits periodical behavior: it shows the highest peak at the natural frequency $f_0 = 0.01489$ Hz and its harmonic, of lesser height, at frequencies $f_n = nf_0$, for integers $n \geq 2$

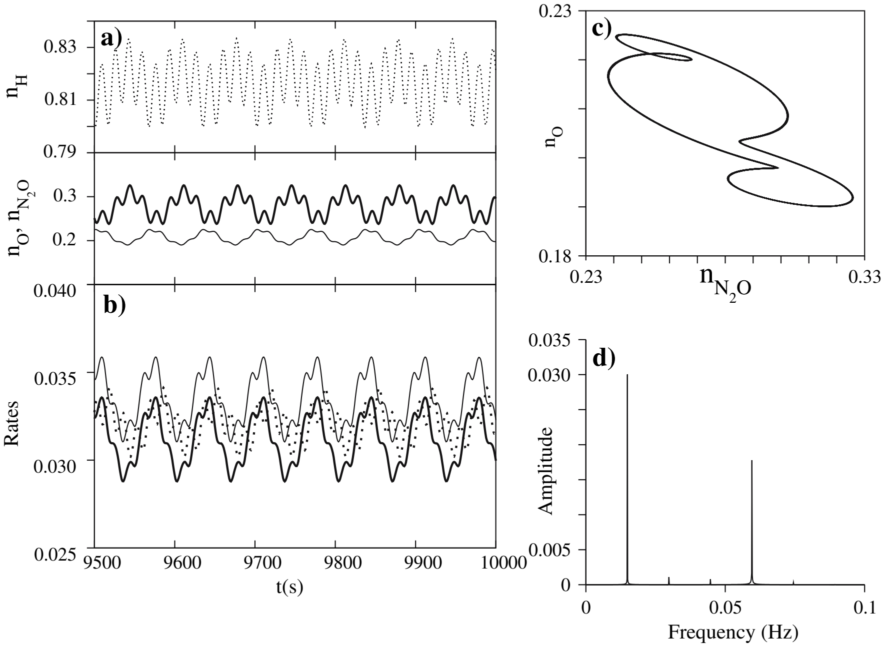

Fig. 8 Forced oscillations P4 at the natural frequency f_0 obtained for the case (iii), $A = B$ and $\varphi = 0$, with $A = 0.2$ and with the imposed frequency $f = 4f_0$. (**a**) Time series of coverages n_H (dashed line), n_{N_2O} (thick line) and n_O (thin line), (**b**) Time series of the rates of dissociation of N_2O (thin line), of adsorption-desorption of N_2O (dashed line) and of formation of H_2O (thick line), (**c**) Stable limit cycle, (**d**) Discrete Fourier spectrum. The system exhibits periodical behavior: it shows the highest peak at the natural frequency $f_0 = 0.01489$ Hz and its harmonic, of lesser height, at frequencies $f_n = nf_0$, for integers $n \geq 2$. The external frequency (4° peak) is the harmonic highest followed by the peaks 2°, 3° and 5°

the external frequency f appear, (4) Figure 10, for $A = B$, $\varphi = \pi/2$, with $f = 6f_0 = 0.08934$ Hz, and $A = 0.9$, oscillations P1 at the external frequency f are obtained. These figures include the time series of the coverage of N_2O, O and H, the reaction rate for the formation of H_2O, for the dissociation of N_2 and for the adsorption–desorption of N_2O, and the stable limit cycles corresponding to the periodical oscillations obtained and the discrete frequency spectra obtained by the conventional technique of the Fourier transform.

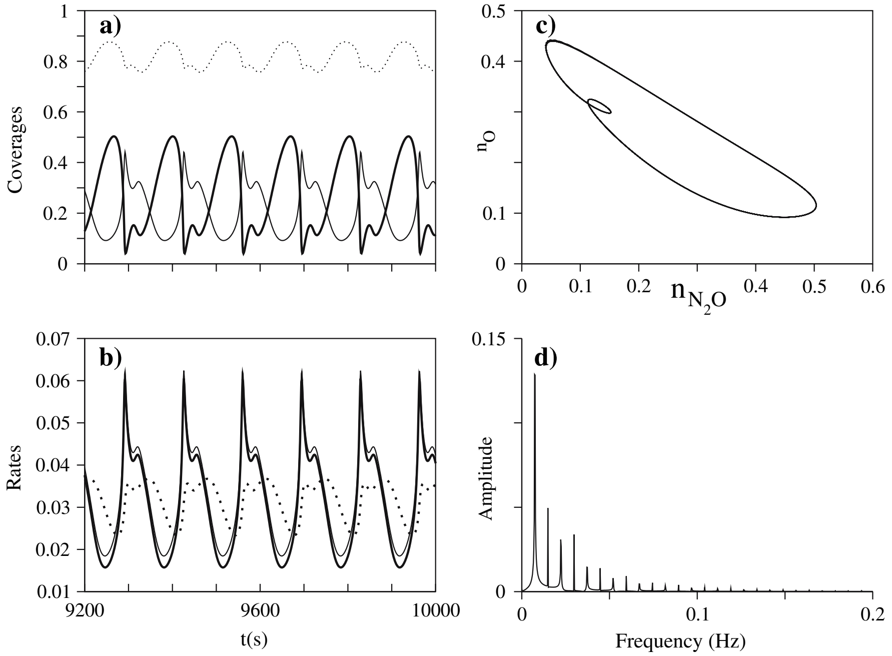

Fig. 9 Forced oscillations P2 at the imposed frequency f obtained for the case (iv), $A = B$ and $\varphi = \pi/2$, with $A = 0.3$ and the imposed frequency $f = 0.5f_0$. (**a**) Time series of coverages n_H (dashed line), n_{N_2O} (thick line) and n_O (thin line), (**b**) Time series of the rates of dissociation of N_2O (thin line), of adsorption-desorption of N_2O (dashed line) and of formation of H_2O (thick line), (**c**) Stable limit cycle, (**d**) Discrete Fourier spectrum. The system exhibits periodical behavior: it shows the highest peak at the imposed frequency $f = 0.007445$ Hz and its harmonic, of lesser height, at frequencies $f_n = f_{n-1} + 0.5f_0$, for integers $n \geq 2$

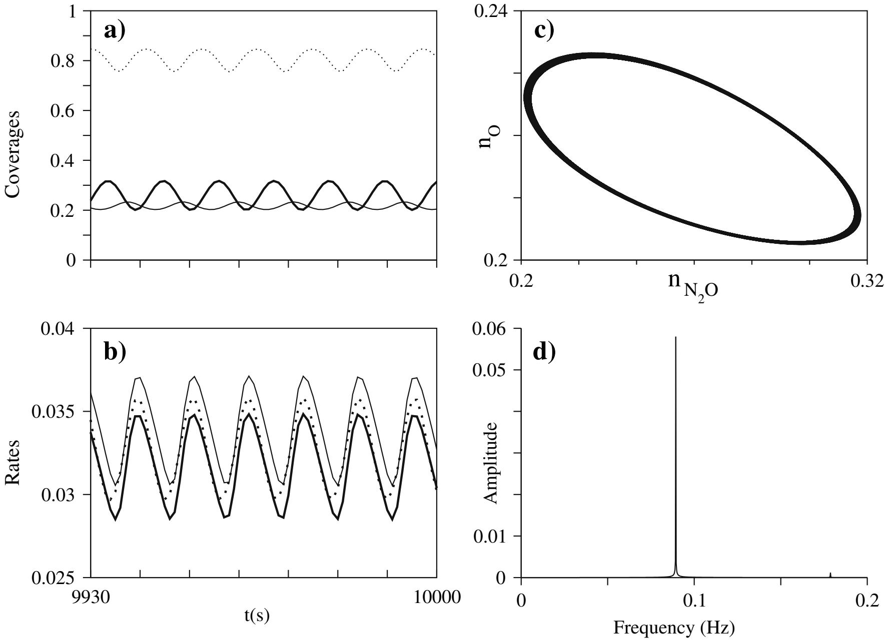

Fig. 10 Forced oscillations P1 at the imposed frequency f obtained for the case (iv), $A = B$ and $\varphi = \pi/2$, with $A = 0.9$ and with the imposed frequency $f = 6f_0$. (**a**) Time series of coverages n_H (dashed line), n_{N_2O} (thick line) and n_O (thin line), (**b**) Time series of the rates of dissociation of N_2O (thin line), of adsorption-desorption of N_2O (dashed line) and of formation of H_2O (thick line), (**c**) Stable limit cycle, (**d**) Discrete Fourier spectrum. The system exhibits periodical behavior: the fundamental frequency corresponds to the peak $f_1 = 0.08936$ Hz, the value 0.17871 being its harmonic

In Figs. 7 and 10 it can be clearly seen that oscillations of $N_2(g)$ (time series at the bottom) are in counter-phase with the oscillations of N_2O (ads) (time series at the top), as it is observed experimentally. Besides there is a slight delay of the maxima of the oscillation of $H_2O(g)$ in relation to the maxima of the oscillations of $N_2(g)$ (time series at the bottom). These results agree with the general behavior of the oscillatory system periodically perturbed in which, for certain values of the parameters characterizing the study of the perturbed oscillatory reaction, the forced system has an oscillatory behavior at the imposed frequency similar to that of the autonomous system at the natural frequency.

4 Conclusions

To sum up, from the MF model of Peskov et al., which simulates the oscillatory behaviour observed experimentally in the heterogeneous catalytic reaction $N_2O + H_2$ on

Ir(110), we have demonstrated that stability of the natural oscillations with regard to periodical perturbations is considerably sensitive to the kind of perturbation. So, perturbations of two variables convert easily autonomous oscillations to oscillations P1 with the imposed frequency. However, perturbations of one variable are much less efficient. This conclusion is in line with the results obtained earlier in Ref. [7].

The greater or smaller sensitiviness of the natural oscillations with regard to sinusoidal perturbations with two parameters ($A = B$) or with one parameter ($A \neq 0$, $B = 0$ or $A = 0$, $B \neq 0$), respectively, can be explained taking into account that in the case of the non-perturbed kinetics the oscillatory window (in the space of the parameters which govern the model) is relatively narrow. Perturbations of one variable correspond mainly to the movement inside the oscillatory window and, therefore, the stability of the natural oscillations is relatively high. On the contrary, perturbations of two variables can easily lead the system to areas which are far from the domain of the natural oscillations and convert these in oscillations P1 at the imposed frequency for an amplitude of the perturbations that is relatively small. Finally, we indicate that the method applied here and the results obtained are general ones and can be applied to other models exhibiting kinetic oscillations.

Acknowledgement This work is partially supported by Junta de Andalucía (FQM-122).

References

1. Zhdanov VP (2004) Surf Sci Rep 55:1
2. Carabineiro SA, Nieuwenhuys BE (2001) Surf Sci 495:1
3. Peskov NV, Slinko MM, Carabineiro SAC, Nieuwenhuys BE (2003) Chem Sustainable Dev 11:221
4. Peskov NV, Slinko MM, Carabineiro SAC, Nieuwenhuys BE (2005) Catal Today 105:223
5. Córdoba A, Lemos MC, Jiménez-Morales F (2006) J Chem Phys 124:014707
6. Córdoba A, Lemos MC, Jiménez-Morales F (2006) Phys Rev E 74:016208
7. Zhdanov VP, Kasemo B (2005) Catal Lett 99:199
8. Sales BC, Turner JE, Maple MB (1982) Surf Sci 114:381
9. Scott SK (1991) Chemical chaos. Clarendon Press, Oxford